

## Raman spectrum of cubic boron nitride at high pressure and temperature

Frédéric Datchi\* and Bernard Canny

*Physique des Milieux Condensés, CNRS UMR 7602, Université Pierre et Marie Curie, 4 place Jussieu, 75252 Paris Cedex 05, France*

(Received 24 October 2003; published 6 April 2004)

Raman scattering experiments on cubic boron nitride were performed at simultaneous high-pressure and high-temperature conditions up to 21 GPa and from 300 to 723 K. Neon served as a (quasi)hydrostatic pressure medium. The frequency shift of the TO mode ( $1054\text{ cm}^{-1}$  at 1 atm and 300 K) is found to be a coupled function of pressure and temperature. Different fits, using either a polynomial form or a Grüneisen model, are presented. The Raman data are used to derive values for the isothermal bulk modulus at ambient and high temperatures. The application of this compound as a high-pressure calibrant at high temperatures is also discussed.

DOI: 10.1103/PhysRevB.69.144106

PACS number(s): 63.20.-e

### I. INTRODUCTION

The zinc blende modification of boron nitride, commonly referred as cubic boron nitride (*c*-BN), is the second hardest known material after diamond. For that reason and other outstanding properties like chemical inertness, high temperature stability, wide band gap and low dielectric constant, it has attracted a large interest in both fundamental and applied fields. Examples of important applications include micro-electronic devices and protective coating materials. On the other hand, the existence, as in the case of carbon, of several polymorphs of BN with very different structural and electronic properties has challenged and motivated a large number of theoretical studies.

The study of BN under pressure is of particular relevance since the discovery of the cubic form necessitated the application of large pressure and temperature.<sup>1</sup> Unlike diamond, though, *c*-BN has been shown to be the thermodynamically stable form at ambient conditions.<sup>2,3</sup> The knowledge of the properties of BN at high pressures and temperatures is thus needed to determine the thermal and mechanical stabilities of the different phases. In return, a better control of the synthesis processes may be achieved. Another application is the determination of the stress state of deposited thin films. In this case, Raman-scattering-based techniques were recently shown to be very useful.<sup>4</sup> Raman spectroscopy is also a powerful fundamental tool to determine vibrational and structural properties of the materials.

The Raman spectrum of *c*-BN exhibits two intense peaks at  $1054$  and  $1304.7\text{ cm}^{-1}$  at ambient conditions corresponding to the Brillouin zone center transverse (TO) and longitudinal (LO) optical modes, respectively. Several authors have reported the pressure dependence up to 34 GPa at room temperature<sup>5,6</sup> and the temperature dependence up to 1840 K at room pressure<sup>7,8</sup> of the frequency shift of the modes. However, there are to date no available experimental data at simultaneous high pressure and high temperature conditions.

The present work reports on Raman scattering experiments on *c*-BN in a diamond anvil cell at pressures up to 21 GPa and temperatures from 300 to 723 K. The *c*-BN sample was compressed in neon which acts as a (quasi)hydrostatic medium in this *P*-*T* range. We limited the investigation to the TO mode as the LO mode was hidden by the Raman

scattering from the diamond anvils ( $1332.5\text{ cm}^{-1}$  at ambient conditions) at pressures above  $\approx 5$  GPa. Our results show that the frequency shift of the TO mode is a coupled function of pressure and temperature. From these measurements and the results of previous studies, we calculate values for the isothermal bulk modulus and its first pressure derivative. To our knowledge, this represents the first experimental estimations of these moduli at temperatures above 300 K. Finally, we will present the advantages of *c*-BN as a pressure calibrant at high temperature in a diamond anvil cell.

### II. EXPERIMENTAL PROCEDURE

A small chip of *c*-BN from De Beers<sup>9</sup> (size:  $21 \times 16 \times 10\text{ }\mu\text{m}^3$ ) was placed in the sample chamber of a membrane diamond anvil cell (MDAC), subsequently filled with high-purity neon gas at 150 MPa using a high-pressure loading apparatus.<sup>10</sup> A rhenium foil of 0.2-mm thickness served as the gasket material. A ruby ball and small amount of  $\text{SrB}_4\text{O}_7:\text{Sm}^{2+}$  powder were loaded together with the sample for purpose of pressure measurement. The formulas used for the ambient-temperature pressure dependence of the wavelength shifts of the ruby ( $R_1$ ) and borate (0-0) lines are, respectively ( $P$  in GPa,  $\lambda$  in nm),<sup>11,12</sup>

$$P_{R_1} = \frac{2.74\lambda_0}{7.665} \left[ \left( \frac{\lambda}{\lambda_0} \right)^{7.665} - 1 \right], \quad (1)$$

$$P_{0-0} = 4.032\Delta\lambda \frac{1 + 9.29 \times 10^{-3}\Delta\lambda}{1 + 2.32 \times 10^{-2}\Delta\lambda}. \quad (2)$$

$\lambda_0$  is the wavelength at  $P=1\text{ atm}$ ,  $T=300\text{ K}$  and  $\Delta\lambda = \lambda(P, T) - \lambda_0$ . Here  $\lambda_0 = 694.256\text{ nm}$  for ruby and  $\lambda_0 = 685.373\text{ nm}$  for the borate.

The temperature dependence of the borate line was neglected as it is very small in the explored temperature range.<sup>12</sup> The one of ruby was measured to be  $7.2 \times 10^{-3}\text{ nm/K}$  at room pressure up to 573 K. The estimated error on pressure measurement is less than  $\pm 0.1\text{ GPa}$ , relative to the pressure scales given by Eqs. (1) and (2).

The whole cell was fitted into a cylindrical resistive heater whose temperature is regulated by a controller from Watlow.<sup>13</sup> Heating was done in air. Raman scattering as well

TABLE I. Observed neon melting points.  $T$  is the temperature measured with the thermocouple in K,  $P_{expt}$  is the pressure measured with the borate in GPa, and  $P_{SG}$  is the melting pressure calculated with the Simon-Glatzel law from Ref. 15.

$T$	$P_{expt}$	$P_{SG}$
464.9	9.39	9.23
561.0	12.23	12.19
645.2	14.99	14.99
723.2	17.86	17.73

as luminescence measurements were performed in back-scattering geometry using a T64000 Raman spectrometer (Jobin-Yvon-Horiba,<sup>14</sup>  $f=0.64$  m, 1800 grooves/mm grating, 100  $\mu\text{m}$  entrance slits) coupled to a confocal microscope for collection and a  $\ell\text{N}_2$ -cooled CCD array detector. Excitation was done with the 514.532-nm line from a  $\text{Ar}^+$  laser. The frequency calibration of the spectral range seen by the detector was made before each acquisition using the spectral lines from a neon lamp. The estimated uncertainty in absolute frequency calibration is  $\pm 0.3 \text{ cm}^{-1}$ .

Temperature was measured with a type- $K$  thermocouple cemented to the side of one of the anvils using high-temperature cement. This temperature agreed with that calculated from the wavelength shifts of the ruby and borate lines, as described in Ref. 12, within  $\pm 5$  K up to 573 K. At higher temperature a poorer agreement was observed, certainly due to the strong overlap or the  $R$  lines that make the determination of the  $R_1$  line position less accurate. As an additional check, we measured during the experiment the melting temperature of neon at several pressures from 9.4 to 17.8 GPa. As shown in Table I, the obtained melting points are in excellent agreement with the Simon-Glatzel melting law fitted to data up to 5.5 GPa.<sup>15</sup>

The laser power used for excitation of the luminescence was 4–10 mW, and 39 mW at maximum for Raman measurements (measured at the focal point of the microscope objective outside the MDAC). By comparing the frequency shift of the TO mode measured for various laser powers, we noticed that light absorption by the sample could cause excess heating. This effect was maximal at room pressure (e.g., a 340 K excess heating was observed for a laser power of 39 mW), certainly due to the fact that heat dissipation in air is less effective than when the sample was surrounded by the neon medium in direct contact with the diamond anvils. The laser power was therefore kept below values where excess heating was observed.

All the reported measurements were made with the same  $c\text{-BN}$  sample for optimal consistency. After each pressure increment, the sample temperature was raised successively to 373, 473, 573, 673, and 723 K. The cell was allowed to achieve thermal equilibrium (temperature fluctuations below  $\pm 0.5$  K) before acquisition was started. The collection time varied from 300 to 600 s.

### III. RESULTS

In total, 70 points of measurements were obtained from ambient pressure to 21 GPa. They are gathered in Table II

and shown in Fig. 1. Figure 2 shows the Raman spectrum obtained at 20.6 GPa and 723 K. A pseudo-Voigt function was fitted to the Raman spectra to determine the peak positions. No attempt was made to obtain the true linewidth from the observed one as we are mainly interested in the frequency shift. The measured full widths at half maximum spread from 7.9 to 11.8  $\text{cm}^{-1}$ .

#### A. Ambient pressure results

The temperature dependence of the TO mode frequency shift at ambient pressure was previously measured by two groups: Alvarenga *et al.*,<sup>7</sup> on the one hand, made measurements from 300 to 1600 K and obtained a linear shift with temperature of  $-0.038(2) \text{ cm}^{-1}/\text{K}$  (as through all the text, numbers in parentheses stand for the standard deviations and apply to the last digit); Herchen and Capelli,<sup>8</sup> on the other hand, reported measurements from 300 to 1840(60) K, and found a nonlinear behavior well described by the relation

$$\nu_{TO}(P=0, T) = \nu_0 + aT + bT^2, \quad (3)$$

with  $\nu_0 = 1060.6(14) \text{ cm}^{-1}$ ,  $a = -0.0100(27) \text{ cm}^{-1} \text{ K}^{-1}$  and  $b = -1.42(12) \times 10^{-5} \text{ cm}^{-1} \text{ K}^{-2}$ . Our results, although limited to 723 K, also show a nonlinear behavior with temperature and agree very well with those of Herchen and Capelli if we rescale them to take into account the difference in the zero temperature frequency shift [i.e., in our case  $\nu_0 = 1058.3(1) \text{ cm}^{-1}$ ].

The temperature dependence of the frequency shift can be viewed as the sum of two contributions, one resulting from a pure volume effect due to thermal expansion and the second, referred as the self-energy term, corresponding to the frequency shift at constant volume.<sup>16</sup> This is formally expressed as

$$\Delta \nu_{TO}(P=0, T) = \left. \frac{\partial \nu}{\partial V} \right|_T \Delta V + \left. \frac{\partial \nu}{\partial T} \right|_V \Delta T. \quad (4)$$

The frequency shift  $\nu_V(T)$  due to thermal expansion alone may be calculated using the isothermal mode Grüneisen parameter  $\gamma$  and the linear thermal expansion coefficient  $\alpha$  through

$$\nu_V(T) = \nu_0 \exp\left(-3\gamma \int_0^T \alpha(T) dT\right). \quad (5)$$

This calculation was done by Refs. 7 and 8, using  $\gamma = 1.5$  for the TO mode. This value however is too high as shown by Aleksandrov *et al.*,<sup>6</sup> who found  $\gamma = 1.188(2)$  from simultaneous measurements of the Raman frequency and specific volume up to 34 GPa. We have recalculated  $\nu_V(T)$  using the latter value for  $\gamma$  and the measurements of  $\alpha(T)$  up to 1250 K at 1 atm by Slack and Bartram.<sup>17</sup> Table III shows the resulting decomposition of the observed thermal shift into the two contributions. Unlike the conclusions of Ref. 7, we find that the pure temperature effect is dominant up to 1250 K. We stress, however, that this result is strongly dependent on the values of  $\nu_0$  and  $\alpha$  which are both poorly constrained (to our knowledge, no Raman data exists below

TABLE II. Experimental results.  $T$  is the thermocouple temperature in K;  $P$  is the pressure measured with the borate in GPa;  $\nu_{TO}$  and  $\sigma_{TO}$  are, respectively, the frequency shift of the TO mode and its standard deviation in  $\text{cm}^{-1}$  obtained by fitting a pseudo-Voigt function to the experimental spectra;  $P_{calc}$  is the pressure calculated with Eq. (11).

$P$	$T$	$\nu_{TO}$	$\sigma_{TO}$	$P_{calc}$	$P$	$T$	$\nu_{TO}$	$\sigma_{TO}$	$P_{calc}$
0.00	300.0	1053.93	0.10	-0.09	9.71	573.0	1080.56	0.06	9.72
0.00	373.0	1052.43	0.20	-0.11	10.00	673.0	1078.46	0.07	9.96
0.00	473.0	1050.17	0.13	-0.11	10.24	723.0	1077.38	0.08	10.13
0.00	573.0	1048.17	0.27	0.05	10.25	300.0	1087.39	0.07	10.21
0.00	673.0	1045.45	0.13	0.08	10.53	373.0	1087.54	0.07	10.58
0.00	723.0	1043.91	0.41	0.08	10.97	473.0	1086.67	0.09	10.88
2.45	300.0	1062.25	0.50	2.41	11.81	723.0	1082.69	0.10	11.78
2.65	373.0	1062.06	0.50	2.75	12.37	573.0	1089.01	0.08	12.34
2.98	473.0	1061.06	0.50	3.09	12.63	723.0	1085.05	0.10	12.52
3.33	573.0	1059.64	0.50	3.41	12.65	673.0	1086.91	0.07	12.59
3.59	673.0	1057.55	0.50	3.63	12.78	300.0	1095.09	0.10	12.68
3.77	723.0	1056.51	0.50	3.79	12.96	373.0	1095.07	0.10	12.97
3.93	300.0	1066.90	0.10	3.83	13.34	473.5	1094.58	0.09	13.37
4.11	373.0	1066.65	0.10	4.14	13.69	573.3	1093.20	0.08	13.66
4.35	300.0	1068.24	0.15	4.23	14.34	723.0	1090.39	0.11	14.21
4.47	573.0	1063.39	0.15	4.52	14.42	673.0	1092.89	0.09	14.48
4.48	473.0	1066.02	0.11	4.57	15.17	300.0	1102.40	0.11	15.06
4.67	373.0	1068.16	0.13	4.59	15.36	373.6	1102.24	0.13	15.28
4.78	673.0	1060.92	0.13	4.64	15.71	473.6	1101.79	0.08	15.67
5.01	473.0	1067.60	0.13	5.04	16.12	573.4	1100.66	0.08	16.03
5.30	723.0	1061.27	0.42	5.22	16.85	673.0	1100.19	0.11	16.81
5.36	573.0	1066.34	0.17	5.40	17.38	473.6	1106.91	0.11	17.33
5.50	300.0	1072.49	0.09	5.54	17.56	373.6	1109.11	0.07	17.53
5.75	673.0	1064.30	0.30	5.65	17.81	723.0	1101.52	0.11	17.80
5.98	723.0	1063.48	0.35	5.88	17.96	573.5	1106.49	0.12	17.92
6.55	373.0	1074.46	0.13	6.51	18.02	672.8	1104.01	0.10	18.05
6.85	473.0	1073.95	0.13	6.96	18.23	300.0	1111.97	0.08	18.24
7.10	673.0	1068.82	0.13	7.01	19.27	300.0	1114.97	0.08	19.25
7.22	573.0	1072.47	0.10	7.25	19.36	373.7	1114.20	0.11	19.22
7.41	673.0	1069.99	0.11	7.37	19.61	723.0	1107.36	0.11	19.71
7.52	723.0	1068.64	0.10	7.45	19.63	474.0	1113.51	0.10	19.49
7.65	300.0	1078.83	0.13	7.51	19.94	573.0	1112.42	0.10	19.85
8.04	373.0	1079.32	0.15	8.01	20.41	300.0	1118.40	0.07	20.42
9.25	723.0	1074.27	0.13	9.17	20.59	722.6	1109.91	0.12	20.55
9.33	473.0	1081.88	0.08	9.39	20.99	673.0	1112.95	0.09	20.99

300 K). As a matter of fact, it is most likely that the zero temperature frequency shift of the TO mode is lower than the one extrapolated from 300 K, which would diminish the pure temperature-induced shift. For comparison, we repeated this analysis for the LTO mode of diamond, for which experimental data on the Raman shift and  $\alpha$  are available from about 15 K to 1900 K.<sup>17-19</sup> In this case also, a pure temperature effect is needed to reproduce the frequency shift above 250 K, that raises rapidly to about 50% of the shift at  $T \approx 600$  K.

## B. Ambient temperature results

The room-temperature pressure dependence of the Raman shift of the TO mode was studied up to 8.2 GPa in a 4:1 methanol-ethanol mixture by Sanjurjo *et al.*,<sup>5</sup> on the one hand, and up to 34 GPa in helium by Aleksandrov *et al.*,<sup>6</sup> on the other hand. The former authors found a linear shift of  $3.39(8) \text{ cm}^{-1}/\text{GPa}$ . Our measured frequencies below 10 GPa are well approximated by a linear variation of  $3.27(2) \text{ cm}^{-1}/\text{GPa}$ , in fair agreement with Sanjurjo *et al.*'s value.

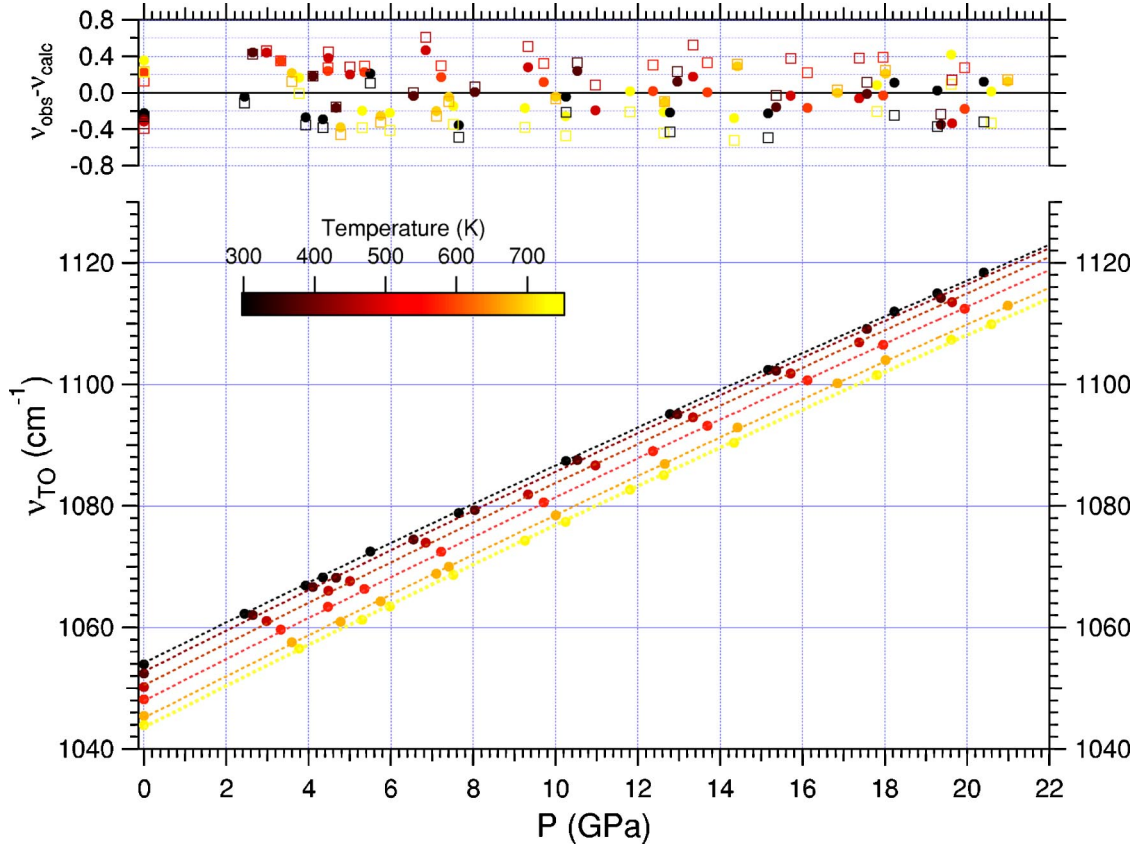


FIG. 1. (Color online) Frequency shift of the TO mode as a function of pressure and temperature. Circles represent experimental data (error bars within the symbol size). The temperature at which the data were collected is indicated by the color scale. Dashed lines show the fit to the data according to Eq. (8), model 2. The top graph shows the difference between experiment and Eq. (8), model 2 (solid circles) or Eqs. (9) and (10) (boxes).

However the frequency shift over the whole pressure range is clearly non-linear and is well reproduced by

$$\begin{aligned} \nu_{TO}(P, 300 \text{ K}) = & 1054.00(14) + 3.33(3)P \\ & - 8.85(150) \times 10^{-3} P^2. \end{aligned} \quad (6)$$

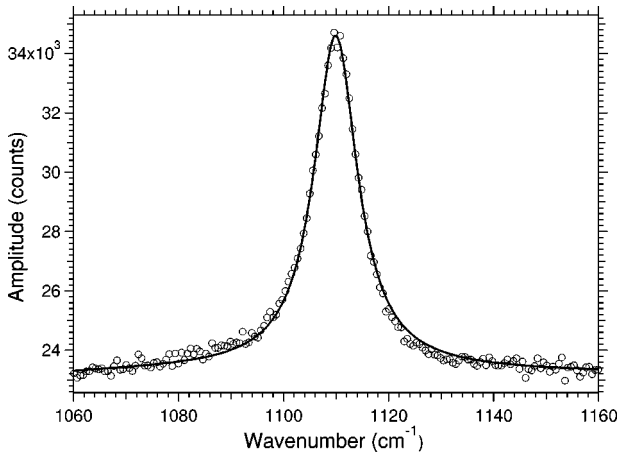


FIG. 2. Raman spectrum of *c*-BN (TO mode) at 20.6 GPa and 723 K (10 min acquisition with 39 mW laser power). The line is a pseudo-Voigt profile fitted to the data points (○).

A direct comparison with Ref. 6 requires us first, to recompute our pressure values, since Aleksandrov *et al.* used a different calibration for the ruby scale. After doing so, we observe a maximum difference between their and our Raman shifts of  $0.7 \text{ cm}^{-1}$ , which is within the mutual uncertainties of the two measurements (Ref. 6 gives an uncertainty of  $0.5 \text{ cm}^{-1}$ ).

From the present measurements of the phonon frequency

TABLE III. Decomposition of the thermal shift of the TO mode at ambient pressure into pure volume and pure temperature effects.  $T$  is in K,  $\Delta \nu_{TO} = \nu_{TO}(T) - \nu_0$ ,  $\Delta \nu_V = \nu_V(T) - \nu_0$  [Eq. (5)] and  $\Delta \nu_T = \nu_{TO}(T) - \nu_V(T)$  are in  $\text{cm}^{-1}$ .

$T$	$\Delta \nu_{TO}$	$\Delta \nu_V$	$\Delta \nu_T$
300	-4.37	-0.47	-3.90
373	-5.87	-0.84	-5.03
473	-8.13	-1.57	-6.56
573	-10.13	-2.57	-7.56
673	-12.85	-3.86	-8.99
723	-14.39	-4.61	-9.78
1000	-24.20 <sup>a</sup>	-9.91	-14.29
1250	-34.69 <sup>a</sup>	-15.76	-18.93

<sup>a</sup>From Ref. 8 [Eq. (3) with  $\nu_0 = 1058.3 \text{ cm}^{-1}$ ].



TABLE IV. Results of the least-squares fit of Eq. (8) to the Raman data. Frequencies are in  $\text{cm}^{-1}$ , pressures in GPa, and temperatures in K.  $\chi^2$  has the usual meaning.

	Model 1	Model 2
$\nu_0$	1058.4(2)	1058.3(4)
$a$	$-9.6(7) \times 10^{-3}$	$-9.3(18) \times 10^{-3}$
$b$	$-1.54(7) \times 10^{-5}$	$-1.54(19) \times 10^{-5}$
$c_0$	3.325(11)	3.07(3)
$c_1$	$2.22(15) \times 10^{-4}$	$1.25(14) \times 10^{-3}$
$c_2$	0	$-1.03(14) \times 10^{-6}$
$d$	$-0.0115(4)$	$-0.0103(4)$
$\chi^2$	590	242

and Ref. 6's value of the mode Grüneisen parameter  $\gamma$ , it is possible to extract the values of the bulk modulus  $B_0$  and its first derivative  $B'_0$ . To do so, we used the first-order Murnaghan equation of state,<sup>20</sup> leading to the following expression for the Raman frequency:

$$\nu_{TO}(P, 300 \text{ K}) = \nu_{TO}(0, 300 \text{ K}) \left( 1 + \frac{B'_0}{B_0} P \right)^{\gamma/B'_0}. \quad (7)$$

A least-squares fit of Eq. (7) to our data leads to  $\nu_{TO}(0, 300 \text{ K}) = 1054.0(1) \text{ cm}^{-1}$ ,  $B_0 = 372(3) \text{ GPa}$  and  $B'_0 = 3.7(2)$ . These values of the moduli are in very good agreement with a direct determination from x-ray volume measurements up to 115 GPa giving  $B_0 = 369(14) \text{ GPa}$  and  $B'_0 = 4.0(2)$ .<sup>21</sup> Aleksandrov *et al.*<sup>6</sup> reported  $B_0 = 382(3) \text{ GPa}$  and  $B'_0 = 4.5(2)$  but, as mentioned above, they used a different pressure calibration for the ruby scale. Brillouin scattering experiments yielded  $B_0 = 400(20) \text{ GPa}$ .<sup>22</sup> The most recent theoretical calculations have given values ranging from 367 to 400 GPa for  $B_0$  and from 3.31 to 3.8 for  $B'_0$  (see Ref. 3, 21, and 23 and references therein).

### C. High-pressure and high-temperature results

Several polynomial expressions were tested to fit our measurements of the TO mode frequency shift over the whole pressure and temperature range covered by the experiment. We found that the data set is best reproduced by the functional form

$$\nu_{TO}(P, T) = \nu_0 + aT + bT^2 + (c_0 + c_1T + c_2T^2)P + dP^2. \quad (8)$$

The resulting parameters of the fit are gathered in Table IV. All parameters were left free to vary except  $a$  and  $b$  which were restricted to vary within the limits of the fit given by Ref. 8 (see Sec. III A). We present the results obtained with either  $c_2$  fixed to zero (model 1) or not (model 2). Model 2 is clearly superior in terms of  $\chi^2$  but model 1 is also found acceptable. Inclusion of higher-order terms in Eq. (8) does not significantly improve the fit. The quality of this fit

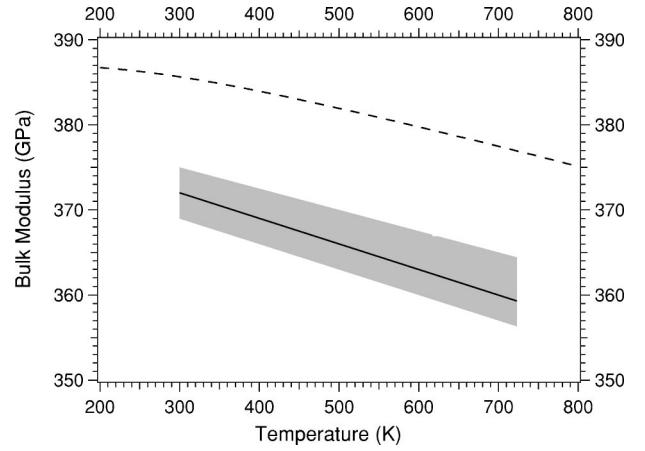


FIG. 3. Temperature dependence of the bulk modulus of *c*-BN. The solid line represents the variation derived from the Raman measurements, with the uncertainty [estimated from the standard deviation of the fit parameters of Eq. (10)] indicated by the hatched region. The dashed line is from the calculations of Albe (Ref. 3) (Debye-Grüneisen model).

can be appreciated from Fig. 1: most data points are reproduced within  $\pm 0.3 \text{ cm}^{-1}$  for model 2 and  $\pm 0.6 \text{ cm}^{-1}$  for model 1.

Equation (8) shows that the frequency shift of the TO mode is a coupled function of pressure and temperature. The shift obtained by summing the ambient-pressure temperature dependence [Eq. (3)] and the ambient-temperature pressure dependence [Eq. (6)] increasingly deviates from the measured one: the difference reaches  $\approx 1.8 \text{ cm}^{-1}$  at the highest *P-T* condition, which is well outside the error bars.

We showed in the previous section that we could obtain values of the bulk modulus and its pressure derivative from the ambient temperature data in very good agreement with other experimental values. To the knowledge of the authors, there is no available experimental data for these moduli at higher temperatures. On the other hand, the variation of  $B_0$  with temperature has been calculated by Albe<sup>3</sup> using first-principle methods and a Debye-Grüneisen theory to determine respectively the static and vibrational parts of the Helmholtz free energy. In order to extract values for  $B_0(T)$  from the present measurements, we make the assumption that the mode Grüneisen parameter is independent of temperature in the range spanned by the experiment. Furthermore, we suppose that the variation of  $B'_0$  with temperature is negligible, and that the one of  $B_0$  can be approximated by a linear function. These assumptions are commonly used and seem reasonable for very hard materials like *c*-BN. We then assume that Eq. (7) can be generalized in the form

$$\nu_{TO}(P, T) = \nu_{TO}(0, T) \left( 1 + \frac{B'_0}{B_0(T)} P \right)^{\gamma/B'_0}, \quad (9)$$

where  $\nu_{TO}(0, T)$  is given by Eq. (3). By fitting the latter expression to the whole Raman data set, we obtain

$$B_0(T) = 372(3) - 0.030(5) \times (T - 300). \quad (10)$$

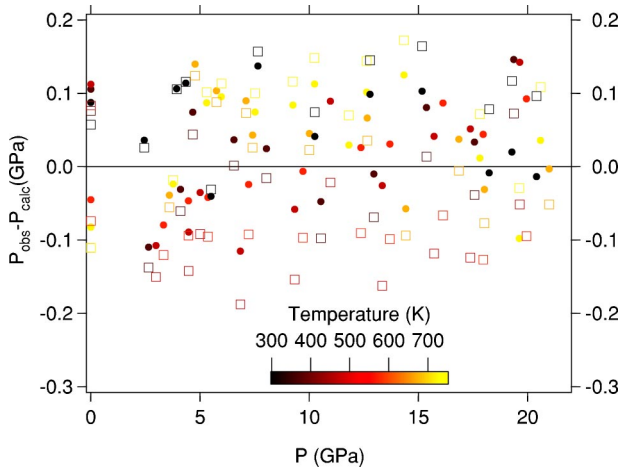


FIG. 4. (Color online) Difference between the measured pressure and the one calculated using Eq. (11) (solid circles) or Eq. (12) (boxes).

This fit gives similar results as Eq. (8), model 1: the residuals remain within  $\pm 0.6 \text{ cm}^{-1}$  (Fig. 1, top graph). The evolution of  $B(T)$  is plotted in Fig. 3 and compared to the calculations of Ref. 3. In both cases, the bulk modulus is seen to decrease with temperature, as expected. Our slope of  $-0.030(5) \text{ GPa K}^{-1}$  is slightly higher than the one from Albe<sup>3</sup> ( $-0.021 \text{ GPa K}^{-1}$  between 300 and 723 K). However, considering the simple model used to describe the thermal effects in Ref. 3, the agreement can be considered very satisfactory. For comparison, the temperature derivative of the bulk modulus of diamond, as measured by ultrasonic methods, is  $-0.010(2) \text{ GPa K}^{-1}$  at 300 K.<sup>24</sup>

#### IV. APPLICATION OF CUBIC BN AS A PRESSURE CALIBRANT

One motivation of this work was to investigate the usefulness of *c*-BN as a pressure calibrant at high temperatures. It is well known that commonly used luminescence gauges such as ruby become increasingly hard to detect and inaccurate at temperatures beyond 750 K, due to line broadening, fall in intensity of the luminescence lines and enhancement of the background level. If no x-ray setup is available to determine pressure from the equation of state of standards like gold, then the use of the Raman activity of *c*-BN is an attractive alternative<sup>25</sup> because (1) it is intense, although much less than the ruby  $R_1$  luminescence line, but still enough to be measured in a reasonable time with standard Raman equipment; (2) it has a small linewidth ( $\approx 3.5 \text{ cm}^{-1}$  at ambient conditions) which increases slowly with temperature;<sup>8</sup> and (3) detectability at high temperatures only depends on how well the thermal emission contributing to the background level is rejected.

Compared to diamond, another good candidate,<sup>18,26</sup> it presents the advantages that (1) the TO mode of *c*-BN is well separated in frequency from the Raman active phonon of diamond ( $1332.5 \text{ cm}^{-1}$  at ambient conditions), and therefore is not masked by the signal from the anvils; and (2) *c*-BN is more chemically inert than diamond, in particular with re-

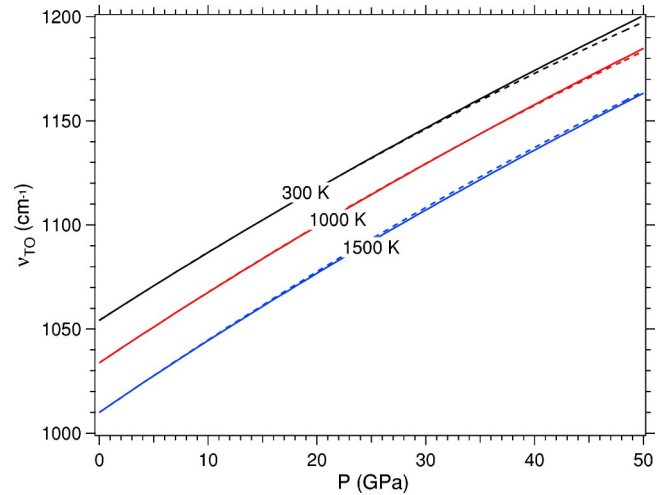


FIG. 5. (Color online) Frequency shift of the TO mode as calculated with Eqs. (8), model 1 (dashed lines), and (9) (solid lines). The experimentally covered range extends up to 21 GPa and 723 K. Temperatures are indicated for each curve.

spect to Fe-, Ni- and Co-containing materials.

Further, *c*-BN is easily available commercially in sizes suitable for diamond anvil cell experiments. Finally, the cubic form of boron nitride is stable over a wide range of pressure and temperature. Apart from the reduced intensity, the main disadvantage compared to luminescence gauges like ruby is that the pressure shift is smaller (about 2.3 times as small as the one of the ruby  $R_1$  line), making the accuracy of pressure determination more sensitive to experimental uncertainties. However this can be partially overcome by using a highly-dispersive set-up and making precise determination of the peak position by least-squares fitting.

The present work can be useful in determining pressure from the measured frequency shift of the TO mode. To this goal, Eq. (8) can be inverted to give

$$P = -\frac{1}{2d} \{A(T) + \sqrt{A(T)^2 + 4d[\nu_{TO}(P,T) - B(T)]}\}, \quad (11)$$

where  $A(T) = c_0 + c_1T + c_2T^2$  and  $B(T) = \nu_0 + aT + bT^2$ .

Table II lists the pressure calculated with Eq. (11) and parameters of model 2. The difference between the measured and calculated pressures is represented in Fig. 4. It is seen that the largest deviation is about 0.15 GPa, showing that relatively accurate pressure reading can be made using this calibrant.

It is well known that empirical polynomial fits have in general poor extrapolating properties. This makes the use of Eqs. (8) and (11) outside the calibration range rather doubtful. In this regard, Eq. (9), resting on more physical grounds, should behave in a better fashion. Inverting the latter relation leads to a “rubylike” formula

$$P = (101.8 - 8.19 \times 10^{-3}T) \left\{ \left[ \frac{\nu_{TO}(P,T)}{\nu_{TO}(0,T)} \right]^{3.074} - 1 \right\}. \quad (12)$$

The difference between experimental pressures and the ones calculated with Eq. (12) is also displayed in Fig. 4.

Although poorer agreement than with Eq. (11) is observed, the difference remains below 0.2 GPa. Figure 5 shows the calculated frequency shifts of the TO mode up to 50 GPa and 1500 K using either Eq. (8), model 1 or Eq. (9). As can be seen, these two expressions have essentially the same behavior. Of course, Raman data at higher pressures and temperatures would be desirable to support the validity of these extrapolations.

## V. CONCLUSIONS

We have presented the results of Raman scattering experiments on *c*-BN in a (quasi)hydrostatic medium up to 21 GPa and from 300 to 723 K. To our knowledge, these are the first reported measurements of the Raman spectra at simultaneous high pressure and high temperature conditions. We have shown that the frequency shift of the TO mode is a coupled function of pressure and temperature and cannot be deduced

from the sole knowledge of the ambient pressure and ambient temperature variations. By using the previously determined value of the Grüneisen parameter of the TO mode and making reasonable assumptions, we were able to derive values for the isothermal bulk modulus in the covered temperature range which are in very good agreement with other experimental or theoretical values. Finally, we emphasized the advantages of *c*-BN as a pressure gauge at high temperature for diamond anvil cell experiments and provided calibration functions which can be used to determine pressure with an accuracy of about 0.15 GPa.

## ACKNOWLEDGMENT

This work was supported by the Commissariat à l'Énergie Atomique under Grant No. 4600035666. We also wish to thank A. Polian for providing the *c*-BN sample and J.-C. Chervin for his help with the neon loading.

\*Email address: fd@pmc.jussieu.fr

<sup>1</sup>R.H. Wentorf, *J. Chem. Phys.* **26**, 956 (1957).

<sup>2</sup>V.L. Solozhenko, *Thermochim. Acta* **218**, 221 (1993).

<sup>3</sup>K. Albe, *Phys. Rev. B* **55**, 6203 (1997).

<sup>4</sup>W.J. Zhang and S. Matsumoto, *Phys. Rev. B* **63**, 073201 (2001).

<sup>5</sup>J.A. Sanjurjo, E. López-Cruz, P.Vogl, and M. Cardona, *Phys. Rev. B* **28**, 4579 (1983).

<sup>6</sup>I.V. Aleksandrov, A.F. Goncharov, S.M. Stishov, and E.V. Yakovenko, *Pis'ma Zn. Éksp. Teor. Fiz.* **50**, 116 (1989) [*JETP Lett.* **50**, 127 (1989)].

<sup>7</sup>A.D. Alvarenga, M. Grimsditch, and A. Polian, *J. Appl. Phys.* **72**, 1955 (1992).

<sup>8</sup>H. Herchen and M.A. Cappelli, *Phys. Rev. B* **47**, 14193 (1993).

<sup>9</sup>De Beers Industrial Diamond Division Ltd., Charters, Sunninghill, Ascot, Berkshire.

<sup>10</sup>B. Couzinet, N. Dahan, G. Hamel, and J.C. Chervin, *High Press. Res.* **23**, 409 (2003).

<sup>11</sup>H.K. Mao, J. Xu, and P.M. Bell, *J. Geophys. Res.* **91**, 4673 (1986).

<sup>12</sup>F. Datchi, R. LeToullec, and P. Loubeyre, *J. Appl. Phys.* **81**, 3333 (1997).

<sup>13</sup>Watlow France S.A.R.L., Z.I. Rue Ampere 95300 Pontoise, France.

<sup>14</sup>Jobin Yvon SAS, 16-18 rue du Canal, 91165 Longjumeau Cedex, France.

<sup>15</sup>W.L. Vos, J.A. Schouten, D.A. Young, and M. Ross, *J. Chem. Phys.* **94**, 3835 (1991).

<sup>16</sup>C. Postmus, J.R. Ferraro, and S.S. Mitra, *Phys. Rev.* **174**, 983 (1968).

<sup>17</sup>G.A. Slack and S.F. Bertram, *J. Appl. Phys.* **46**, 89 (1975).

<sup>18</sup>F. Occelli, P. Loubeyre, and R. LeToullec, *Nat. Mater.* **2**, 151 (2003).

<sup>19</sup>E.S. Zouboulis and M. Grimsditch, *Phys. Rev. B* **43**, 12490 (1991).

<sup>20</sup>F.D. Murnaghan, *Am. J. Math.* **49**, 235 (1937).

<sup>21</sup>E. Knittle, R.M. Wentzcovitch, R. Jeanloz, and M.L. Cohen, *Nature (London)* **337**, 349 (1989).

<sup>22</sup>M. Grimsditch, E.S. Zouboulis, and A. Polian, *J. Appl. Phys.* **76**, 832 (1994).

<sup>23</sup>H.W.L. Alves, J.L.A. Alves, J.L.P. Castineira, and J.R. Leite, *Mater. Sci. Eng., B* **59**, 264 (1999).

<sup>24</sup>H.J. McSkimin and P. Andreatch, *J. Appl. Phys.* **43**, 2944 (1972).

<sup>25</sup>M. Eremets, *High Pressure Experimental Methods* (Oxford University Press, Oxford, 1996).

<sup>26</sup>D. Schiferl, M. Nicol, J.M. Zaug, S.K. Sharma, T.F. Cooney, S.-Y. Wang, T.R. Anthony, and J.F. Fleisher, *J. Appl. Phys.* **82**, 3256 (1997).